

Band structure, Wiener bounds, and coupled surface plasmons in one dimensional photonic crystals

Michael Bergmair, Martin Huber, and Kurt Hingerl^{a)}

Christian Doppler Labor für Oberflächenoptische Methoden, Institut für Halbleiter und Festkörperphysik, Universität Linz, A-4040 Linz, Austria

(Received 22 February 2006; accepted 3 July 2006; published online 23 August 2006)

Recently metallic two and three dimensional photonic crystals (PCs) have been studied with the focus on using such structures in incandescent lighting and thermal photovoltaic applications. They exhibit a metallic band gap for low frequencies as well as structural band gaps. Especially the metallic band gap allows to block the infrared transmission respectively emission. In this letter we show that also the structural simpler one dimensional (1D) system has the same features; furthermore it builds an omnidirectional band gap for the Drude dispersion relation. For the case of a polaritonic system 1D PCs are able to exhibit angle of incidence as well as frequency dependent filter characteristics. The dispersion relation of surface plasmons, extending over adjacent layers is obtained. Propagating states must lie within the Wiener bounds. © 2006 American Institute of Physics. [DOI: 10.1063/1.2338546]

Planck's derivation of thermal radiation has led to quantum mechanics but is also extremely important for applications as lighting and sensing. Recently, thermal radiation from three dimensional (3D) metallic photonic crystals has attracted a lot of attention because it was proposed that thermal radiation from these structures might even exceed the radiation of a blackbody.¹ However, an *ab initio* calculation of the equilibrium thermal emission properties of a photonic crystal assuming Kirchhoff's law has shown that thermal radiation from photonic crystals in equilibrium can exceed only that of a blackbody by means of fluctuations (which vanish by averaging).² The physics of surface plasmons (SPLs) and surface polaritons are investigated since long time^{3,4} and SPLs have highly interesting sensor applications⁵ or enhance the efficiency of light emission.⁶ The objective of this letter is to discuss the band structure and a possible omnidirectional reflectance^{7,8} of one dimensional (1D) metallic photonic crystals (MPCs). Photonic crystals with a real dielectric constant are well known and have been investigated since the end of the 1980s. The periodicity in these structures leads to forbidden frequency bands which can be used to filter or to guide waves with a certain energy. Kuzmiak and Maradudin⁹ were one of the first authors who treated MPC characterized by a frequency dependent and complex dielectric function. This frequency dependence is modeled either as Drude⁹ or as polaritonic like.¹⁰ The solution of the eigenvalue equation yields either a complex frequency ω (interpreted as lifetime) or a complex wave vector k (interpreted as spatial damping). Kuzmiak and Maradudin presented two techniques to calculate the band structure: With plane wave expansion (PWE) the band structure $\omega(k)$ and the fields for 1D, two dimensional, and 3D MPCs can be numerically determined; with a Kronig Penney (KP)-like description $k(\omega)$ is calculated, but with the exception of special arrangements,¹¹ only for 1D MPCs. The results given below are obtained with KP, PWE resulted in an higher computational load. The band structure solutions were also correlated

with transmission matrix calculations. The equation from the KP model is¹²

$$\cos(k_z L) = \cos\left(n_1 \frac{\omega}{c} a_1\right) \cos\left(n_2 \frac{\omega}{c} a_2\right) - \frac{1}{2} \frac{n_1^2 + n_2^2}{n_1 n_2} \sin\left(n_1 \frac{\omega}{c} a_1\right) \sin\left(n_2 \frac{\omega}{c} a_2\right), \quad (1)$$

with n_i as refractive index and a_i as width of the layer with indices $i=1, 2$ describing air or metal. The metallic layers are orientated in the x - y plane and separated by air.

In Fig. 1 the band structure for normal incidence onto a 1D MPC, whose dielectric function is Drude-like

$$\varepsilon(\omega, z) = \begin{cases} 1 - \frac{\omega_p^2}{\omega(\omega + i\gamma)} & \text{in metal} \\ 1 & \text{in air,} \end{cases} \quad (2)$$

is shown. We use the filling factor $f=0.1=a_2/L$, a plasma frequency ω_p , and a damping constant γ as $0.01\omega_p$. This choice is motivated by a plasma frequency in the UV ($\omega_p \sim 10^{15} \text{ s}^{-1}$) and an inverse electron relaxation time $\gamma = 10^{13} \text{ s}^{-1}$. For simplicity we introduce the dimensionless

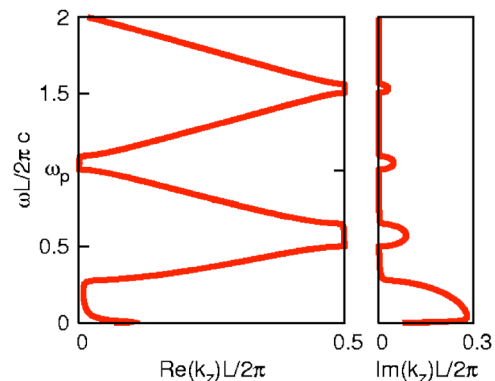


FIG. 1. (Color online) Band structure for normal incidence on a MPC with $f=0.1$ and $\gamma=0.01\omega_p$. The imaginary part corresponds to damping. The metallic band gap extends between zero and $\omega \sim 0.3\omega_p$.

^{a)}Electronic mail: kh@jku.at

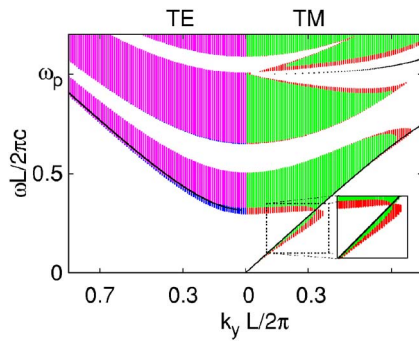


FIG. 2. (Color online) Band structure and allowed states for oblique incidence. In blue (TE) and red (TM) solutions with $\Im(k_z)L/2\pi < 0.01$; in magenta (TE) and green (TM) solutions with $\Im(k_z)L/2\pi < 0.005$ are presented. Wiener bounds are marked by black lines.

variable $\omega L/2\pi c$ which is normalized to 1 at ω_p . In Fig. 1 ω is plotted as a function of the real and imaginary k_z vectors fulfilling the KP equation. Already previous authors^{9,13} have observed a few remarkable effects: (a) propagation through such *infinite* structures becomes allowed even much below ω_p , (b) there is a clear distinction between structural band gaps (second and higher band gaps) and a metallic band gap which extends from $\omega=0$ to $\omega \sim 0.3\omega_p$, and (c) the penetration depth in the metallic band gap is about two to three periods and much less than in the structural band gaps.

These results suggest that 1D MPC structures can be used to filter infrared light in optical applications. Can such filter characteristics be extended to off-axis propagation, too, for obtaining an omnidirectional band gap?^{7,8} To answer this question we calculated the band structure of a 1D MPC for non-normal incidence for TE and TM polarized waves.

The result is shown in Fig. 2. The shaded regions in this plot are solutions of Eq. (1) with a real and positive ω , a real k_y , and a real k_z component [as numerical cutoff we plotted a projection of the solutions $\omega(k_y, k_z)$ with $\Im(k_z)L/2\pi < 0.01$]. Contrary to 1D dielectric PCs with omnidirectional reflection we do not use a light line ($\omega=ck$), because the dielectric function is frequency dependent. However, we plot the Wiener bounds^{14,15} for TE (no screening) as well as for TM (maximum screening) as black lines. The Wiener bounds are upper and lower limits for the effective dielectric function of a composite with a given volume fraction, irrespective of microstructure.

Returning to an omnidirectional band gap, in the case of TE polarized light (E field in plane) no states exist in the metallic band gap. For both polarizations the variation of the cutoff limit $\Im(k_z)$, physically interpreted as inverse penetration depth, is shown by different colors—solutions which exist below the Wiener bounds—for TE, e.g., the blue area must be evanescent.

For TM polarization solutions below the Wiener bounds (Fig. 2) are found in the metallic band gap, plotted in green ($\Im(k_z)L/2\pi < 0.005$), respectively, red ($\Im(k_z)L/2\pi < 0.01$). Further investigation of these solutions shows that they have a vanishing real k_z , i.e., these modes are propagating parallel to the layers. In Fig. 3 the solutions of Eq. (1) with a zero and real k_z component are presented (red). The bars indicate the imaginary part of k_z (norm is given in the inset). This dispersion relation approaches in the limit $k_y \rightarrow \infty$ the one of surface plasmons.¹⁶ It is worth to mention that damping occurs mainly in the direction perpendicular to the layers, the

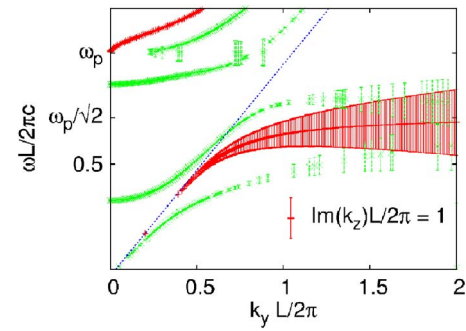


FIG. 3. (Color online) Dispersion of pure surface plasmons in red ($\Re(k_z)=0$) and plasmons propagating with ($\Re(k_z)L/2\pi=0.2$) in green. The vertical bars indicate the damping, norm given by the red bar.

in plane propagation of the SPLs is hardly damped despite the finite γ .

For small k_y , $\omega \ll \omega_p$, and small filling factors the transcendental Eq. (1) reduces for $k_z=0$ to

$$\omega = \frac{ck_y}{\sqrt{\epsilon_{\text{air}}}} \sqrt{1-f}. \quad (3)$$

This relation is shown as blue dashed line in Fig. 3. For a single metal-air surface the low frequency limit is exactly the same except the factor $\sqrt{1-f}$ which takes into account the periodicity of and coupling between metallic layers. For small wavelengths ($k_y \rightarrow \infty$) the condition $\epsilon_{\text{air}} = -\epsilon_{\text{metal}}$ has to be fulfilled (also results from Wiener bounds) and therefore the dispersion has to reach the limit $\omega = \omega_p/\sqrt{2}$ (Fig. 3). The dispersion relation exhibits a band gap between $\omega_p/\sqrt{2}$ and ω_p , as in the case of a single metallic surface, occurring through the common effect of the first structure band gap and the surface plasmon behavior.¹⁶ In Fig. 3 solutions (green) with $\Re(k_z)L/2\pi=0.2$ are shown, representing modes propagating concurrently through the stack and along the layers.

We now turn to the polaritonic dielectric function $\epsilon(\omega) = \epsilon_\infty + (\epsilon_0 - \epsilon_\infty)\omega_T^2/(\omega_T^2 - \omega^2 - i\omega\gamma)$ which yields for bulk material the Reststrahlenbande in the infrared with ω_T as transversal optical frequency. The values of the dielectric function at $\omega=0$ and at $\omega=\infty$ depend on ω_L , the longitudinal optical frequency, via the Lyddane-Sachs-Teller relation $\epsilon_0/\epsilon_\infty = (\omega_L/\omega_T)^2$.

Bulk materials with a polaritonic dielectric function have a band gap between ω_T and ω_L ; in infrared MPCs this band gap is modified as we will see in Figs. 4 and 5. The band structure for normal and oblique incidences in these figures is calculated with $\omega_L L/2\pi c = 1$ and $\omega_T L/2\pi c = 0.62$. The values for ω_T , ϵ_0 , and ϵ_∞ used in Fig. 4 are typical for an ionic crystal as, e.g., BeO (if $L = 8.85 \mu\text{m}$).¹⁰

Some quite interesting phenomena are (a) the largest damping that occurs at the transversal optical frequency which implies (b) that there are again two different types of band gaps—the structure band gaps and the polaritonic band gap (at ω_T) and (c) the PC becomes transparent below ω_L . By choosing different material parameters and/or selecting the appropriate thickness of the layers one can either merge a structure band gap and the polaritonic band gap into a huge one, or construct a band pass, in addition transparent only for a certain angle of incidence. Therefore it is interesting how the band structure changes in the case of oblique incidence. In Fig. 5 again, propagating states can only exist above the Wiener bounds. An interesting feature occurs for the TE case

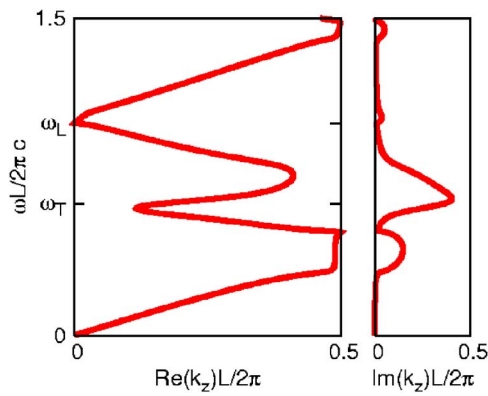


FIG. 4. (Color online) Normal incidence band structure for a polaritonic photonic crystal with $f=0.1$ for $\epsilon_0=7.75$, $\omega_T L/2\pi c=0.62$, and a damping factor of $\gamma=0.132\omega_T$.

around ω_L close to the Wiener bound. These volume states become allowed due to periodicity and have a very small k_z and a dominating k_y component, they propagate almost parallel to the metallic layers. On a single flat surface modes with this polarization cannot exist.

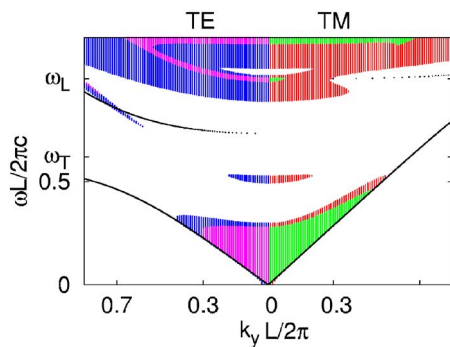


FIG. 5. (Color online) Band structure for polaritonic PCs. In blue (TE) and red (TM) solutions with $\Im(k)L/2\pi < 0.03$; in magenta (TE) and green (TM) solutions with $\Im(k)L/2\pi < 0.01$ are presented. Wiener bounds are marked in black parameters in Fig. 4.

Summarizing we studied 1D MPC under normal and oblique incidences and found a modification of dispersion relations for surface plasmons extending over more than one metallic layer. For polaritonic dispersion relations the interplay between metallic and structure band gaps allows a variety of applications. For both cases, metallic as well as polaritonic PC omnidirectional band gaps exist. The interrelation between Wiener bounds and states propagating along the surface is clarified.

The authors are grateful to Johann Messner from the Linz Supercomputer Department for numerous support as well as CPU time grants and to Heinz Seyringer from Photon Technologies. They gratefully acknowledge an EC grant (3D Nanoprint).

¹P. Weiss, see article on <http://www.sciencenews.org/articles/20031004/bob9.asp> (2003).

²C. Luo, A. Narayanaswamy, G. Chen, and J. Joannopoulos, *Phys. Rev. Lett.* **93**, 213905 (2004).

³H. Raether, *Surface Plasmons on Smooth and Rough Surfaces and on Gratings* (Springer, Berlin, 1988), Vol. 3, p. 4.

⁴V. Agranovich, *Surface Polaritons* (North-Holland, Amsterdam, 1982), Vol. 1, p. 10.

⁵A. Stepanov, J. Krenn, H. Ditlbacher, A. Hohenau, A. Drezet, B. Steinberger, A. Leitner, and F. Aussenegg, *Opt. Lett.* **30**, 893 (2005).

⁶R. Pariella, *Appl. Phys. Lett.* **87**, 111104 (2005).

⁷D. Chigrin, A. Lavrinenko, D. Yarotsky, and S. Gaponenko, *J. Lightwave Technol.* **17**, 2018 (1999).

⁸J. Winn, Y. Fink, S. Fan, and J. Joannopoulos, *Opt. Lett.* **23**, 1573 (1998).

⁹V. Kuzmiak and A. Maradudin, *Phys. Rev. B* **55**, 7427 (1997).

¹⁰A. Rung and C. Ribbing, *Phys. Rev. Lett.* **92**, 123901 (2004).

¹¹S. Kawakami, *J. Lightwave Technol.* **20**, 1644 (2002).

¹²P. Yeh, *Optical Waves in Layered Media* (Wiley, New Jersey, 1988), p. 125.

¹³X. Xu, Y. Xi, D. Han, X. Liu, J. Zi, and Z. Zhu, *Appl. Phys. Lett.* **86**, 091112 (2005).

¹⁴D. Aspnes, *Phys. Rev. B* **25**, 1358 (1982).

¹⁵O. Wiener, *Abh. Math-Phys. Kl. Königl. Saechs. Ges.* **32**, 509 (1912).

¹⁶K. Sakoda, *Optical Properties of Photonic Crystals* (Springer, Berlin, 2004), p. 161.